Antennas in Reception

Laboratory 07 Manual

Prof. Aluizio Prata

1 Laboratory Objective

In a previous laboratory we studied in detail wire antennas when they operate transmitting energy. This is only half of the picture though, since in any communication link we also need to have antennas operating receiving electromagnetic energy. With this in mind, in this laboratory we will continue our study of antennas, this time considering their operation as they receive electromagnetic energy.

As always, we will approach the material at hand from both the theoretical and the experimental viewpoints. Again here we will first go over the theory involved, then perform some numerical simulations, and finally we will confirm our predictions through detailed experiments. To be successful in this laboratory you need to have studied in detail the material covered in Chap. 11 of our textbook[1], and also study the theory presented ahead.

As you have already observed multiple times, each laboratory relies heavily on the material learned in previous classes and also all previous laboratories. More than ever this is true with the current laboratory; to be able to handle this laboratory you will absolutely need to have successfully completed the previous laboratory that dealt with wire antennas operating in transmission. This is a cardinal requirement, since both laboratories complement and rely heavily on each other (for instance, you will be augmenting and modifying the Matlab code that you developed for the previous laboratory). *If then for any reason you did not successfully complete the Antennas in Transmission laboratory, you will need to go back and do so.* The current laboratory will also take advantage of some basic material that should be familiar to you from previous linear algebra courses.

As a result of this laboratory you will need to generate and submit a laboratory report for grading. The report should have each of its sections and subsections numbered according to this laboratory manual, and be a detailed document with all your derivations, calculations, design efforts, measurement results, conclusions, drawings, plots, relevant photos of all constructed components (to showcase your very important high-frequency craftsmanship), and printouts of any developed software.

Note that, to maximize the learning experience, the laboratory has been designed to be carried out individually, hence each person in the class received their own individual lab kits. Consequently, the experiment and the corresponding report has to be done completely individually.

Document version: January 8, 2024, at 11:44 o'clock

[1] D. K. Cheng, *Field and Wave Electromagnetics*, Second edition, Addison-Wesley Pub. Co., 1989.

2 Mutual Impedance between Two Linear Dipole Antennas

In a general communication link two antennas are used to transfer electromagnetic energy using the intervening space as a waveguide. Now that we understand how a single antenna operates when it is transmitting energy, in this section we will consider in detail how a communication link between two antennas is achieved. With this in mind consider two dipole antennas (labeled 1 and 2) located in free space and separated by a distance ℓ, as shown in Fig. 1. Note that for drawing simplicity the two antennas are depicted parallel to each other, with the distance ℓ measured between their centers and perpendicular to the dipoles' arms. Although this particular orientation of the two dipole antennas relative to each other maximizes the power transfer, since the peak of their radiation patterns are aimed at each other, the link will still work, but less efficiently, if the two antennas are not perfectly aligned. The antennas 1 and 2 have lengths $2h_1$ and $2h_2$ and diameters $2a_1$ and $2a_2$, respectively, and it will be assumed that the diameters of the two antennas are such that $2a_1 \ll \lambda_0$ and $2a_2 \ll \lambda_0$.

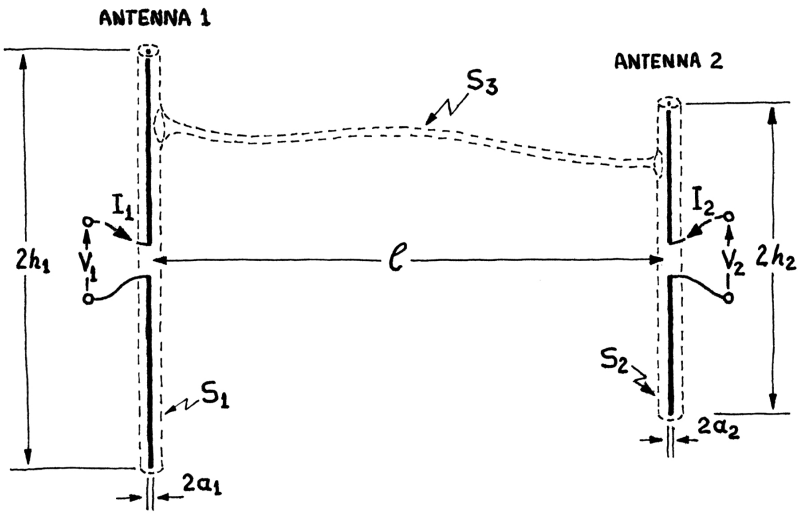

Figure 1: Geometry for determining the mutual impedance between two dipole antennas

The communication link shown in Fig. 1 is clearly a two-port network and hence we know that its behavior is governed by the circuit equations

$$V_1 = Z_{11}\, I_1 + Z_{12}\, I_2\,, \tag{1}$$

$$V_2 = Z_{21}\, I_1 + Z_{22}\, I_2\,, \tag{2}$$

where the impedance matrix elements (i.e., Z_{11}, Z_{12}, Z_{21}, and Z_{22}) must be determined using Maxwell's Equations, as opposed to Kircchoff's voltage and current laws, since they are originating from the air link (i.e., electromagnetic wave coupling) between the two antennas.

In order to determine how much energy is produced in the terminals of antenna 2 (or 1) when antenna 1 (or 2) is transmitting we need to determine the electromagnetic coupling between the two antennas. To accomplish this we will basically proceed as in

the previous laboratory, and rely on the complex Poynting theorem. To this effect note that a single closed mathematical surface $S_1+S_2+S_3$ is shown snugly enclosing the two antennas of Fig. 1, and this surface will be used in the derivation below. Observe that a snug surface is needed in order to capture all the relevant reactive energy stored in the space surrounded by the two antennas.

The terminal voltages and currents of Eqs. 1 and 2 (i.e., V_1, I_1 and V_2, I_2) are associated with whatever circuits are connected to the antennas; they are either being produced by transmitters connected to the antennas, or they are being produced by the signals received by the antennas. In either case, time-averaged complex powers

$$P_1 = \frac{1}{2}\, V_1 I_1^* \,, \tag{3}$$

$$P_2 = \frac{1}{2}\, V_2 I_2^* \,, \tag{4}$$

are being delivered to antennas 1 and 2, respectively. Note that, according to the polarities shown in Fig. 1, the real parts of the above P_1 and P_2 will automatically come out negative when the antennas are receiving energy. Assuming that the antennas have negligible losses, the power delivered to the terminals of the two antennas (i.e., P_1+P_2) must be equal to the power crossing the surface $S_1+S_2+S_3$ shown in Fig. 1, and hence we can use the Poynting vector to write

$$\frac{1}{2}\, V_1 I_1^* + \frac{1}{2}\, V_2 I_2^* = \frac{1}{2}\int\limits_{S_1} \vec{E} \times \vec{H}^* \cdot \vec{ds} + \frac{1}{2}\int\limits_{S_2} \vec{E} \times \vec{H}^* \cdot \vec{ds} + \frac{1}{2}\int\limits_{S_3} \vec{E} \times \vec{H}^* \cdot \vec{ds} \,. \tag{5}$$

Before proceeding we need to discuss in more detail the role of the conductors present in the above geometry. It turns out that if you remove all the electric conductors of the geometry, but somehow mathematically leave all the flowing electric currents unchanged and in place, it can be shown that the electromagnetic field present remains everywhere unchanged. In practice the electric conductors are then "only" needed to provide a medium for the currents to flow along the desired paths (currents simply can't be made to flow along any desired path in vacuum). However, mathematically (i.e., on paper) conductors are not needed after the currents are flowing. Hence, and as long as you keep every current the same in your theoretical model (again, this is of course only possible on paper), you can remove all the conductors, and all the electromagnetic fields, with their associated currents and voltages, will remain unchanged. Conceptually this is a very a useful result, since it provides us with an equivalent geometry that is free space everywhere (no conductors to worry about). From now on we will then assume that we did this to the geometry of Fig. 1 and we are only considering its free-space equivalent.

Returning to Eq. 5, let's now assume that the surface S_3 that connects the two antennas is basically a long straw with negligible diameter. In this case the surface area of the straw is negligible and consequently its corresponding integral contribution to Eq. 5 is negligible and can be discarded. Hence, observing that the electromagnetic field of the geometry is basically a superposition of the fields radiated individually by antennas 1 and 2, namely $\vec{E}_1, \vec{H}_1$ and $\vec{E}_2, \vec{H}_2$, respectively, Eq. 5 becomes

$$V_1 I_1^* + V_2 I_2^* = \int\limits_{S_1} (\vec{E}_1 + \vec{E}_2) \times (\vec{H}_1 + \vec{H}_2)^* \cdot \vec{ds} + \int\limits_{S_2} (\vec{E}_1 + \vec{E}_2) \times (\vec{H}_1 + \vec{H}_2)^* \cdot \vec{ds} \,. \tag{6}$$

Now, substituting Eqs. 1 and 2 on the left side of Eq. 6 and expanding the right side yields

$$\begin{aligned} I_1 I_1^* Z_{11} + I_2 I_1^* Z_{12} + I_1 I_2^* Z_{21} + I_2 I_2^* Z_{22} = & \int_{S_1} \vec{E}_1 \times \vec{H}_1^* \cdot \vec{ds} + \int_{S_1} \vec{E}_1 \times \vec{H}_2^* \cdot \vec{ds} \\ & + \int_{S_1} \vec{E}_2 \times \vec{H}_1^* \cdot \vec{ds} + \int_{S_1} \vec{E}_2 \times \vec{H}_2^* \cdot \vec{ds} \\ & + \int_{S_2} \vec{E}_1 \times \vec{H}_1^* \cdot \vec{ds} + \int_{S_2} \vec{E}_1 \times \vec{H}_2^* \cdot \vec{ds} \\ & + \int_{S_2} \vec{E}_2 \times \vec{H}_1^* \cdot \vec{ds} + \int_{S_2} \vec{E}_2 \times \vec{H}_2^* \cdot \vec{ds} \,, \end{aligned} \tag{7}$$

which can be rewritten as

$$\begin{aligned} I_1 I_1^* Z_{11} + I_2 I_1^* Z_{12} + I_1 I_2^* Z_{21} + I_2 I_2^* Z_{22} = & \, I_1 I_1^* \left[\int_{S_1} \frac{\vec{E}_1}{I_1} \times \frac{\vec{H}_1^*}{I_1^*} \cdot \vec{ds} + \int_{S_2} \frac{\vec{E}_1}{I_1} \times \frac{\vec{H}_1^*}{I_1^*} \cdot \vec{ds} \right] \\ & + I_2 I_1^* \left[\int_{S_1} \frac{\vec{E}_2}{I_2} \times \frac{\vec{H}_1^*}{I_1^*} \cdot \vec{ds} + \int_{S_2} \frac{\vec{E}_2}{I_2} \times \frac{\vec{H}_1^*}{I_1^*} \cdot \vec{ds} \right] \\ & + I_1 I_2^* \left[\int_{S_1} \frac{\vec{E}_1}{I_1} \times \frac{\vec{H}_2^*}{I_2^*} \cdot \vec{ds} + \int_{S_2} \frac{\vec{E}_1}{I_1} \times \frac{\vec{H}_2^*}{I_2^*} \cdot \vec{ds} \right] \\ & + I_2 I_2^* \left[\int_{S_1} \frac{\vec{E}_2}{I_2} \times \frac{\vec{H}_2^*}{I_2^*} \cdot \vec{ds} + \int_{S_2} \frac{\vec{E}_2}{I_2} \times \frac{\vec{H}_2^*}{I_2^*} \cdot \vec{ds} \right]. \end{aligned} \tag{8}$$

Observing that the electromagnetic field $\vec{E}_1, \vec{H}_1$ is proportional to I_1 and the electromagnetic field $\vec{E}_2, \vec{H}_2$, is proportional to I_2, we can see that each of the four terms inside brackets depend only on the geometry, and not on the currents. Hence we see that

$$Z_{11} = \int_{S_1} \frac{\vec{E}_1}{I_1} \times \frac{\vec{H}_1^*}{I_1^*} \cdot \vec{ds} + \int_{S_2} \frac{\vec{E}_1}{I_1} \times \frac{\vec{H}_1^*}{I_1^*} \cdot \vec{ds} \,, \tag{9}$$

$$Z_{12} = \int_{S_1} \frac{\vec{E}_2}{I_2} \times \frac{\vec{H}_1^*}{I_1^*} \cdot \vec{ds} + \int_{S_2} \frac{\vec{E}_2}{I_2} \times \frac{\vec{H}_1^*}{I_1^*} \cdot \vec{ds} \,, \tag{10}$$

$$Z_{21} = \int_{S_2} \frac{\vec{E}_1}{I_1} \times \frac{\vec{H}_2^*}{I_2^*} \cdot \vec{ds} + \int_{S_1} \frac{\vec{E}_1}{I_1} \times \frac{\vec{H}_2^*}{I_2^*} \cdot \vec{ds} \,, \tag{11}$$

$$Z_{22} = \int_{S_2} \frac{\vec{E}_2}{I_2} \times \frac{\vec{H}_2^*}{I_2^*} \cdot \vec{ds} + \int_{S_1} \frac{\vec{E}_2}{I_2} \times \frac{\vec{H}_2^*}{I_2^*} \cdot \vec{ds} \,. \tag{12}$$

The last integrals in each of the above equations turn out to be negligible when compared to the first integrals. On Eq. 9 it is negligible because one is integrating the Poynting vector produced by antenna 1 over a closed volume surrounding antenna 2, and the power that is going into S_2 is equal to the power leaving S_2 (the energy is pretty much just passing through). For similar reasons the last integral in Eq. 12 is zero. With respect to the last integral of Eq. 10, since the diameter of antenna 2 is very small in relation to the wavelength, on the surface S_2 the $\vec{E}_2$ is everywhere in the same direction (please take a good look at the upcoming Eq. 22) and the same is true for $\vec{H}_1$. This causes the integration over half the surface S_2 to cancel the integration over the remaining half, causing then the last integral of Eq. 10 to be zero. The same type of behavior also causes the last integral in Eq. 11 to be zero. We then have

$$Z_{11} = \frac{1}{I_1 I_1^*} \int\limits_{S_1} \vec{E}_1 \times \vec{H}_1^* \cdot \vec{ds}\,, \tag{13}$$

$$Z_{12} = \frac{1}{I_2 I_1^*} \int\limits_{S_1} \vec{E}_2 \times \vec{H}_1^* \cdot \vec{ds}\,, \tag{14}$$

$$Z_{21} = \frac{1}{I_1 I_2^*} \int\limits_{S_2} \vec{E}_1 \times \vec{H}_2^* \cdot \vec{ds}\,, \tag{15}$$

$$Z_{22} = \frac{1}{I_2 I_2^*} \int\limits_{S_2} \vec{E}_2 \times \vec{H}_2^* \cdot \vec{ds}\,. \tag{16}$$

If you look carefully at the all details of the above derivation you will conclude that Eqs. 13 – 16 are very general; they are actually valid for any two antennas, provided that they have circuit terminals (they are not valid just for linear dipoles). By the way, the results provided by Eqs. 13 and 16 should already look familiar, as they were already derived in the previous laboratory; they are the dipoles' input impedances.

Observe that once you have the parameters of the impedance matrix in hand (determined using analysis, experiments, or both), other matrix representations can be derived from them. For instance, the S-parameters that VNAs routinely measure can be obtained from the above impedance parameters using[2]

$$S_{11} = \frac{(Z_{11}-Z_0)(Z_{22}+Z_0) - Z_{12}Z_{21}}{(Z_{11}+Z_0)(Z_{22}+Z_0) - Z_{12}Z_{21}}\,, \tag{17}$$

$$S_{12} = \frac{2\,Z_{12}Z_0}{(Z_{11}+Z_0)(Z_{22}+Z_0) - Z_{12}Z_{21}}\,, \tag{18}$$

$$S_{21} = \frac{2\,Z_{21}Z_0}{(Z_{11}+Z_0)(Z_{22}+Z_0) - Z_{12}Z_{21}}\,, \tag{19}$$

$$S_{22} = \frac{(Z_{11}+Z_0)(Z_{22}-Z_0) - Z_{12}Z_{21}}{(Z_{11}+Z_0)(Z_{22}+Z_0) - Z_{12}Z_{21}}\,. \tag{20}$$

As seeing in a previous laboratory, the physical arrangement of Fig.1 can then be represented by the equivalent T-circuit shown in Fig. 2, where the corresponding

[2]See for example D. M. Pozar, *Microwave Engineering*, Third ed., John Wiley & Sons, Inc., 2005, pag. 187.

impedances are given by Eqs. 13 – 16. In this section we will be mainly focused on Eq. 15, which provides the coupling between dipoles 1 and 2. This Z_{21}, which by reciprocity is equal to Z_{12}, is the term that makes possible for the two antennas to communicate with each other.

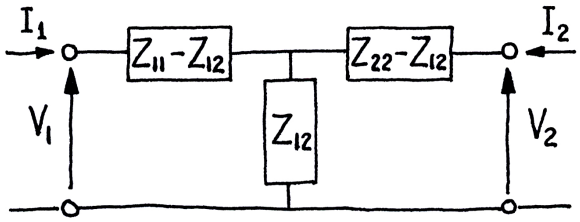

Figure 2: Equivalent circuit of the reciprocal link between two antennas

Note that the $\vec{E}_1$ of Eq. 15 is the electric field produced by antenna 1 along antenna 2 (i.e., the electric field radiated by the current that is flowing on antenna 1), and $\vec{H}_2^*$ is the complex conjugate of the magnetic field along antenna 2 (i.e., the complex conjugate of the magnetic field radiated by the current that is flowing on antenna 2). These two fields can be calculated by properly using Eqs. 22 and 23 given below[3], which give the field radiated by a thin dipole antenna at any distance, when a sinusoidal current

$$I(z) \approx I_m \, \sin[\beta_0(h - |z|)] \tag{21}$$

is flowing on its arms. Even though you have already used these equations in a previous laboratory, for completeness they are being provided again here.

$$\vec{E}(P) = \frac{j\,\eta_0\,I_m}{4\pi}\left\{ -\,\hat{r}\,\frac{1}{r}\left[\,2\,e^{-j\beta_0 R_0}\cos\theta_0\,\cos(\beta_0 h) - e^{-j\beta_0 R_1}\cos\theta_1 - e^{-j\beta_0 R_2}\cos\theta_2\right]\right.$$
$$\left. +\,\hat{z}\left[2\,\frac{e^{-j\beta_0 R_0}}{R_0}\,\cos(\beta_0 h) - \frac{e^{-j\beta_0 R_1}}{R_1} - \frac{e^{-j\beta_0 R_2}}{R_2}\right]\right\}, \tag{22}$$

$$\vec{H}(P) = \frac{-j\,I_m}{4\pi}\,\hat{\phi}\,\frac{1}{r}\left[\,2\,e^{-j\beta_0 R_0}\cos(\beta_0 h) - e^{-j\beta_0 R_1} - e^{-j\beta_0 R_2}\right]. \tag{23}$$

Recall again that in these equations the observation point P is located by the cylindrical coordinates (r, ϕ, z), the fields are described using the corresponding cylindrical unit vectors (i.e., $\hat{r}$, $\hat{\phi}$, and $\hat{z}$), the dipole has length $2h$, negligibly small radius (the radius a is not even present in these equations), the variables R_0, R_1, R_2, θ_0, θ_1, and θ_2 are given by (see Fig. 3)

$$R_0 = \sqrt{r^2 + z^2}\,, \tag{24}$$
$$R_1 = \sqrt{r^2 + (z-h)^2}\,, \tag{25}$$
$$R_2 = \sqrt{r^2 + (z+h)^2}\,, \tag{26}$$
$$\cos\theta_0 = z/R_0\,, \tag{27}$$
$$\cos\theta_1 = (z-h)/R_1\,, \tag{28}$$
$$\cos\theta_2 = (z+h)/R_2\,, \tag{29}$$

[3]E. C. Jordan *Electromagnetic Waves and Radiating Systems*, Prentice-Hall, Inc., April 1960, pag. 320–324.

and the current amplitude I_m is related to the dipole input current I_i through

$$I_m = \frac{I_i}{\sin(\beta_0 h)} \,. \tag{30}$$

With these equations we currently have all the means to use Eq. 15 to determine the Z_{21} of two dipoles, located in close proximity or far away from each other.

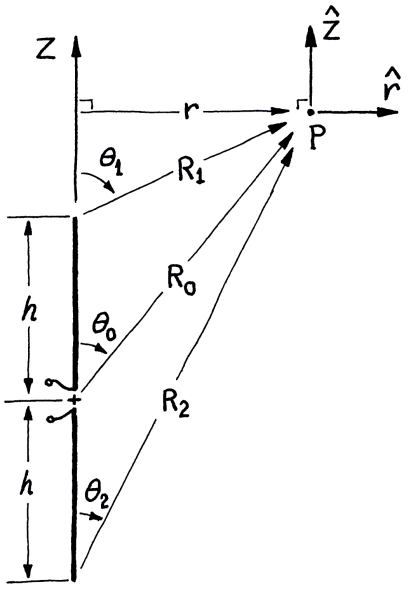

Figure 3: Parameters associated with the near-zone field of a straight dipole

Before proceeding it is important to be able to clearly and unambiguously differentiate between the two cylindrical coordinate systems that will need to be independently associated with antennas 1 and 2, as the geometry shown in Fig. 3 will need to be used to calculated the fields radiated by both antennas 1 and 2. We will do this by using corresponding subscripts: r_1, ϕ_1, z_1 and r_2, ϕ_2, z_2 will refer to the cylindrical coordinates of antennas 1 and 2, respectively.

The cylindrical surface S_2 has top and and bottom caps located at $z = \pm h_2$, respectively. Hence the surface S_2 is constituted of three separate surfaces. However, if the antenna 2 diameter $2a_2$ is small, which is usually the case when $2a_2 \ll \lambda_0$, the integration over these top and bottom caps will yield a relatively small contribution to the total integral value, and hence can be safely neglected when compared with the integration over the side surface of the cylinder S_2. In this case $\vec{ds} = \hat{r}_2\, dz_2\, r_2\, d\phi_2$ and Eq. 15 becomes

$$Z_{21} = \frac{1}{I_1 I_2^*} \int_0^{2\pi} \int_{-h_2}^{+h_2} \Big(\vec{E}_1\Big|_{r_1=\ell} \times \vec{H}_2^*\Big|_{r_2=a_2} \Big) \cdot \hat{r}_2\, dz_2\, a_2\, d\phi_2 \,, \tag{31}$$

where we have assumed that $\ell + a_2 \approx \ell$, since a_2 is being assumed to be very small. Now, since from Eqs. 22 and 23 we see the amplitude of the vector $\vec{E}_1\Big|_{r_1=\ell} \times \vec{H}_2^*\Big|_{r_2=a_2}$ is independent of ϕ_2,

$$Z_{21} = \frac{2\pi a_2}{I_1 I_2^*} \int_{-h_2}^{+h_2} \Big(\vec{E}_1\Big|_{r_1=\ell} \times \vec{H}_2^*\Big|_{r_2=a_2} \Big) \cdot \hat{r}_2\, dz_2 \,. \tag{32}$$

Equation 32 provides the desired result for the mutual impedance between two dipole antennas. To use it one needs to know the electromagnetic fields $\vec{E}_1|_{r_1=\ell}$ and $\vec{H}_2^*|_{r_2=a_2}$ that are radiated by dipoles 1 and 2 on the surface of the dipole 2, respectively (i.e., surface with $r_2 = a_2$). Whenever $2a_2 \ll \lambda_0$, a very good approximation for these two fields is provided by Eqs. 22 and 23.

There is an alternative way to write Eq. 32 that you may find a bit more convenient. To derive it observe from Eqs. 22 and 23 that $\vec{E} = \hat{r}E_r + \hat{z}E_z$ and $\vec{H} = \hat{\phi}H_\phi$, and hence Eq. 32 can be rewritten as

$$Z_{21} = \frac{-2\pi a_2}{I_1 I_2^*} \int_{-h_2}^{+h_2} E_{1z_2}|_{r_1=\ell} \; H^*_{2\phi_2}\big|_{r_2=a_2} dz_2 \,. \tag{33}$$

There is yet another alternative way to rewrite this last equation, which yields the form most commonly found in the literature. To obtain it first recall Ampere's law, namely

$$\oint_C \vec{H} \cdot \vec{d\ell} = j\omega\epsilon_0 \int_{S_c} \vec{E} \cdot \vec{ds} + \int_{S_c} \vec{J} \cdot \vec{ds} \,, \tag{34}$$

where for the application at hand the contour C will be assumed to be a circle of radius a_2 enclosing antenna 2, with center at the coordinate axis z_2, and the surface S_c is then the surface enclosed by this circle. Recalling again from Eq. 23 that $\vec{H}_{2\phi_2} = \hat{\phi}_2 \, H_{2\phi_2}$ we can write

$$2\pi a_2 H_{2\phi_2}\Big|_{r_2=a_2} = j\omega\epsilon_0 \int_{S_c} \vec{E}_2 \cdot \vec{ds} + \int_{S_c} \vec{J}_2 \cdot \vec{ds} \,. \tag{35}$$

Now, observing that the first term on the right side of Eq. 35 is negligibly small and

$$\int_{S_c} \vec{J}_2 \cdot \vec{ds} = I_2(z_2) \,, \tag{36}$$

where $I_2(z_2)$ is the current flowing on antenna 2 (given by Eq. 21), we obtain

$$2\pi a_2 H_{2\phi_2}\Big|_{r_2=a_2} = I_2(z_2) \,, \tag{37}$$

With this last result Eq. 33 becomes

$$Z_{21} = \frac{-I^*_{m2}}{I_1 I_2^*} \int_{-h_2}^{+h_2} E_{1z_2}\Big|_{\text{on antenna 2}} \sin[\beta_0(h_2 - |z_2|)] \, dz_2 \,, \tag{38}$$

where $2h_2$ and I_{m2} are the length and current amplitude of dipole 2, respectively, and E_{1z_2} is the $\hat{z}_2$ component of the field produced by the dipole 1 along the dipole 2.

Observe that the cylindrical integration surface $S_1 + S_2$ was intentionally made snug with the two dipole antennas' arms (see Fig. 1). This is required to capture all the reactive power present in the space surrounding the two antennas (this reactive power is responsible for the reactive part of the antenna mutual impedance Z_{21}). There is a bit of energy stored in both the electric and magnetic fields that exist at the antennas' feed point regions (in the regions with $z_1, z_2 \approx 0$, where the two antennas' arms come together and are connected to the transmission lines). In other words, there is some reactive power present on the approximately parallel-plate capacitors and wire inductances that exist at the antennas' feed points. This reactive power is not being captured by Eq. 38,

since any fringe field effects present in the $z_1, z_2 \approx 0$ regions are being ignored and also the integrations only capture the reactive power outside $S_1 + S_2$. If for any reason these parasitic reactive power are deemed relevant to the communication link operation (perhaps because the antennas' terminals are excessively close to each other), they then need to be accounted for separately, by properly adding the effects of the stray inductances L_f and capacitances C_f.

Let's now apply the above results to understand, calculate, and measure the performance of an electromagnetic link between two identical monopoles over ground planes.

1. Augment your previously developed Matlab code to use Eq. 38 to calculate and plot the transmission coefficient S_{21} between two dipole antennas, in addition to the S_{11} computation.

   Since the calculation of S_{21} is very similar to the calculation of S_{11}, pretty much all you have to do is duplicate and modify your previously developed S_{11} code to also perform the S_{21} calculation.

   Using for antennas 1 and 2 the 600 MHz monopole over ground plane that you designed, constructed, and measured in a previous laboratory, separated by a distance $\ell = 500$ mm, calculate the corresponding S_{21} over the 50 kHz to 1000 MHz frequency range and provide the corresponding $|S_{21}|$ (in dB) and $\angle S_{21}$ (in deg) plots.

   Note that, according to the $2D^2/\lambda_0$ far-zone criterion, the $\ell = 500$ mm separation is more than sufficient to place antennas 1 and 2 well in the far zone of each other. However, your Matlab code does not require the two antennas to be in the far-zone of each other; it is capable of accurately calculating S_{21} even if the two antennas are very close to each other.

2. Construct antenna 2 by duplicating the hardware you did for antenna 1 in a previous laboratory. Then put the two monopoles side by side, separated by a distance $\ell = 500$ mm (see Fig. 4). This will constitute the communication link that you will be measuring.

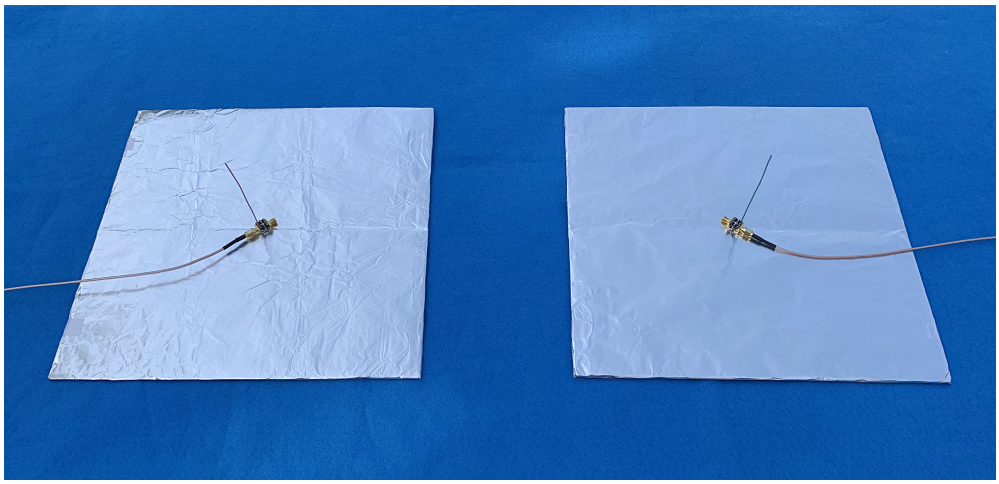

Figure 4: Communication link between two monopoles, with $\ell = 500$ mm

Because you are going to be precisely measuring the signal that is received by antenna 2 when antenna 1 is transmitting, and comparing it with your predictions, it is very important that you minimize interference caused by reflections from surrounding objects. For good measurement accuracy you should then keep objects removed from your two antennas by at least a few wavelengths. Particularly troublesome are large flat surfaces near your communication link, as they can produce strong interfering reflections.

Note that, if you put the two antennas on top of a flat ground, you will have an unaccounted for very large flat surface near your communication link, and its effect will depend on the nature of the ground (i.e., dry, wet, paved, rebar reinforced, etc.). However, at our frequencies dry cemented pavements are usually quite transparent and therefore their effect is negligible. Nevertheless, if you experience significant disagreements between theory and measurements, causing you to become suspicious of the ground impact, simply put your link on top of either a wood table or wood chairs, and this should remove your suspicions.

3. Measure the S_{11} and S_{21} of your two antennas over the 50 kHz to 1000 MHz frequency range and provide the corresponding $|S_{11}|$ and $|S_{21}|$ (in dB), and $\angle S_{11}$ and $\angle S_{21}$ (in deg) plots. Typical plots of the results that can be expected are provided in Fig. 5 (the measurements were conducted with the two antennas resting on top of a dry cemented pavement). Note that these plots include the undesirable effects of the SMA-DIP8-SMA test fixture parasitic reactances, but you will be handling these effects in the next section.

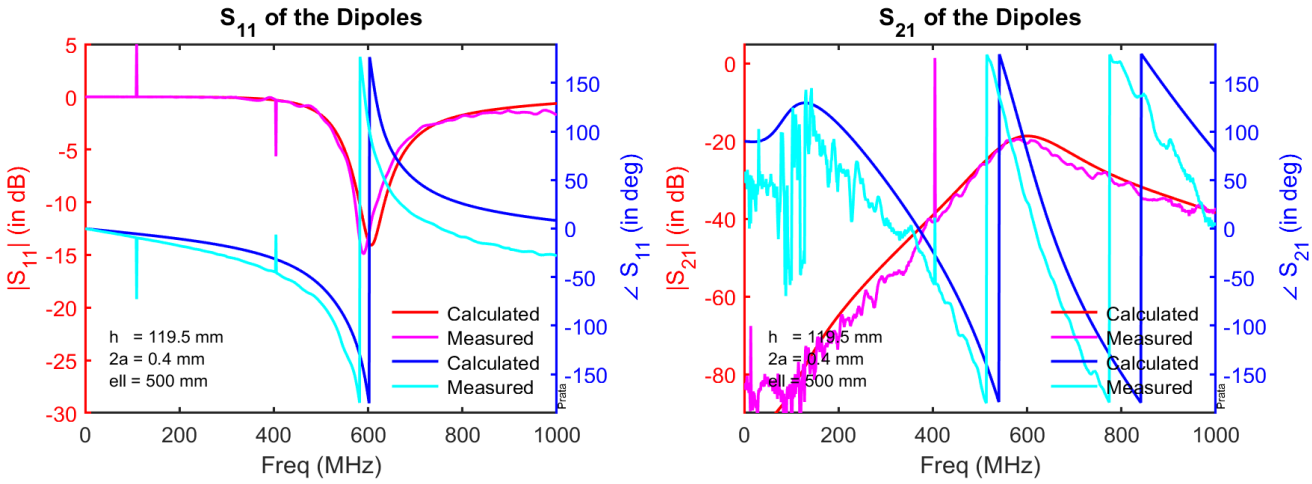

Figure 5: Typical monopole's link embedded S-parameter results

Make sure to compare the predicted and measured results and discuss any relevant details observed. Also make sure to explain why the communication is stronger at the 600 MHz design frequency of your two antennas.

3 De-Embedding the Effect of the Test Fixture

Although reasonable good agreement between theory and experiment should have been obtained between your calculated and measured results (in the previous section), any impact of the test fixture parasitic reactances have so far been ignored. In a previous laboratory we de-embedded the effects of these reactances from the S_{11} and observed that they caused a significant change on the antenna impedance. It is then only natural to wonder how these parasitic reactances are also impacting the measured S_{21}.

In this section we will address the problem of how to de-embed undesired parasitic effects from all the measured scattering parameters in a systematic general way, and not only from just the S_{11}, as we did in a previous laboratory. To do this we will be relying on linear algebra techniques.

A convenient general way to handle de-embedding is through the use of two-port circuits' transmission matrices (also called in the literature by $ABCD$ matrices), namely

$$V_1 = T_{11}\, V_2 + T_{12}\, I_2' \,, \tag{39}$$

$$I_1 = T_{21}\, V_2 + T_{22}\, I_2' \,, \tag{40}$$

instead of the impedance matrices that we have been using up to now. In these equations T_{11}, T_{12}, T_{21}, and T_{22} are the transmission matrix elements, and V_1, I_1 and V_2, I_2 are voltages and currents that are identical to the ones used in the impedance matrix (i.e., Eqs. 1 and 2). Note however that Eqs. 39 and 40 use instead I_2', which is related through I_2 through $I_2' = -I_2$. The very useful difference between the transmission and impedance matrices is that, in the transmission matrix, the port 1 variables (i.e., V_1 and I_1) and the port 2 variables (i.e., V_2 and I_2') are now on the left and right sides of the equal signs, respectively. This rearrangement makes transmission matrices more convenient for handling de-embedding tasks than other matrix representations (such as impedance or scattering matrices). The reason behind this is that it is very easy to determine the transmission matrix of a chain connection of several networks; because all the parameters of port 2 are conveniently located on the right side of the equal sign in Eqs. 39 and 40, all one needs to do is sequentially multiply the individual transmission matrices of each network in the chain. How this property works in our favor will become clear as we proceed, so please read on.

As previously mentioned, conversion formulas between all the various linear circuit matrix representations are available in the technical literature. But particularly useful for the de-embedding task at hand are the conversion formulas between S- and T-parameters, namely[4]

$$T_{11} = \frac{(1+S_{11})(1-S_{22}) + S_{12}S_{21}}{2S_{21}} \,, \tag{41}$$

$$T_{12} = Z_0\, \frac{(1+S_{11})(1+S_{22}) - S_{12}S_{21}}{2S_{21}} \,, \tag{42}$$

[4]See for example D. M. Pozar, *Microwave Engineering*, Third ed., John Wiley & Sons, Inc., 2005, pag. 187.

$$T_{21} = \frac{1}{Z_0}\,\frac{(1-S_{11})(1-S_{22})-S_{12}S_{21}}{2S_{21}}\,, \tag{43}$$

$$T_{22} = \frac{(1-S_{11})(1+S_{22})+S_{12}S_{21}}{2S_{21}}\,, \tag{44}$$

and vice-verse

$$S_{11} = \frac{T_{11}+T_{12}/Z_0-T_{21}Z_0-T_{22}}{T_{11}+T_{12}/Z_0+T_{21}Z_0+T_{22}}\,, \tag{45}$$

$$S_{12} = \frac{2\,(T_{11}T_{22}-T_{12}T_{21})}{T_{11}+T_{12}/Z_0+T_{21}Z_0+T_{22}}\,, \tag{46}$$

$$S_{21} = \frac{2}{T_{11}+T_{12}/Z_0+T_{21}Z_0+T_{22}}\,, \tag{47}$$

$$S_{22} = \frac{-T_{11}+T_{12}/Z_0-T_{21}Z_0+T_{22}}{T_{11}+T_{12}/Z_0+T_{21}Z_0+T_{22}}\,. \tag{48}$$

We know that in general $S_{12} = S_{21}$ for reciprocal circuits. But notice that the above Eqs. 42 and 43 clearly show that in general $T_{12} \neq T_{21}$, even for reciprocal circuits. However, and as an alternative property, Eqs. 46 and 47 show that, for a reciprocal circuit, the determinant of the transmission matrix $[T]$ is equal to 1; in other words

$$\det[T] = T_{11}T_{22} - T_{12}T_{21} = 1\,. \tag{49}$$

Let's now return to the task of de-embedding the measured S-parameters of the link between the two monopoles from the undesired SMA-DIP8-SMA test fixture parasitic reactances. We know that, instead of measuring the desired S-parameters, we have instead measured the S-matrix $[S^e]$ of the entire circuit shown in Fig. 6 (the superscript e stands for embedded), where the box has the desired unadulterated S-matrix $[S]$ of the link between the two antennas (note the direction of the current I_2', on port 2). Taking advantage of our recent acquired transmission matrix knowledge, to de-embed $[S^e]$ we will work instead with the corresponding embedded transmission matrix $[T^e]$ and redraw the measured circuit as a chain of three T-matrices. What was measured

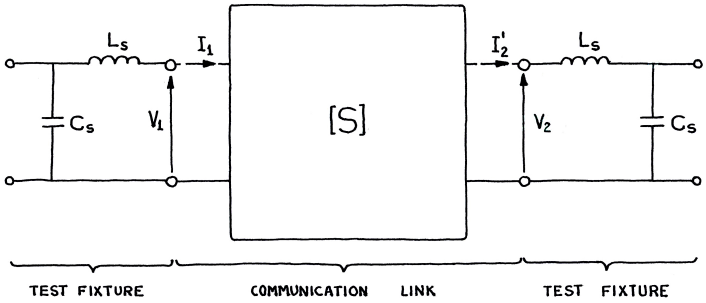

Figure 6: Measured communication link equivalent circuit

then was the matrix $[T^e]$, which is related to the desired de-embedded transmission matrix $[T]$ through

$$[T^e] = [T^{(1)}] \times [T] \times [T^{(2)}]\,, \tag{50}$$

where the multiplication signs denote matrix multiplications, and $[T^{(1)}]$ and $[T^{(2)}]$ are the transmission matrices of the test fixture parasitic circuits connected to ports 1 and 2 of the VNA, given by

$$[T^{(1)}] = \begin{bmatrix} 1 & X_L \\ B_C & 1 + X_L B_C \end{bmatrix} \tag{51}$$

and

$$[T^{(2)}] = \begin{bmatrix} 1 + X_L B_C & X_L \\ B_C & 1 \end{bmatrix}, \tag{52}$$

respectively. The X_L and B_C used in the above equations are the reactance and susceptance associated with L_S and C_S, namely $X_L = j\omega L_s$ and $B_C = j\omega C_s$, respectively.

Now observe that, if both sides of Eq. 50 are multiplied from the left by $[T^{(1)}]^{-1}$ and from the right by $[T^{(2)}]^{-1}$, where the minus subscripts indicate the corresponding inverse matrices, one has

$$[T^{(1)}]^{-1} \times [T^e] \times [T^{(2)}]^{-1} = [T^{(1)}]^{-1} \times [T^{(1)}] \times [T] \times [T^{(2)}] \times [T^{(2)}]^{-1}. \tag{53}$$

Finally, recalling that the product of any matrix by its inverse satisfies the commutative property and is equal to a unitary matrix, we obtain the desired de-embedded transmission matrix $[T]$ result, namely

$$[T] = [T^{(1)}]^{-1} \times [T^e] \times [T^{(2)}]^{-1}. \tag{54}$$

Equation 54 provides a convenient way to de-embed our measurements, since $[T^e]$ can be obtained from the measured $[S^e]$ using Eqs. 41 – 44 and the required two inverses can be readily obtained from Eqs. 51 and 52 using the easily derived and readily available formula for the inverse of a two-by-two matrix. Namely, if an arbitrary transmission matrix $[A]$ is equal to

$$[A] = \begin{bmatrix} a & b \\ c & d \end{bmatrix} \tag{55}$$

then its inverse is

$$[A]^{-1} = \begin{bmatrix} d & -b \\ -c & a \end{bmatrix}, \tag{56}$$

where we have already taken advantage of the fact that the determinant of transmission matrices of reciprocal networks is equal to 1.

The above material provides a convenient systematic way to de-embed measured S-parameters. In it we took advantage of the previously acquired knowledge of the circuit that describes the parasitic reactances of the SMA-DIP8-SMA test fixture (provided by Eqs. 51 and 52), since it was already available. Note however that, for other types of embedding networks, we would have used instead their corresponding transmission matrices for $[T^{(1)}]$ and $[T^{(2)}]$, and these could even have been matrices derived from S-parameter measurements. Our method is then very general and powerful, and does not even require an equivalent circuit for the embedding networks. However, you should not get carried away by its capabilities, as it is always preferable to calibrate out undesirable effects than to de-embed them, since a well-thought and carefully implemented calibration invariably yields better measurement accuracy.

The NanoVNA-F does not have intrinsic de-embedding capabilities in its firmware (you then have to code your own de-embedding algorithm). Other much more expensive commercially available VNAs do though, and it is based in the material that you have just learned.

We will now use your recently acquired knowledge to de-embed the measured results of the previous section. With this in mind, provide answers to the items below.

1. Derive Eqs. 51 and 52.

2. Derive Eq. 56.

3. Augment the Matlab code that you obtained in the previous section to de-embed the measurements made on the link between the two monopoles.

   Note that Matlab is a software originally developed to conveniently handle linear algebra (i.e., matrices). Because of this it already has pretty much all the functions required for linear algebra as intrinsic functions (e.g., calculation of matrix inverses). In fact, when you use the simple product operator between two matrices (i.e., the asterisk, without a preceding dot) Matlab automatically performs the product of the two matrices. You can then handle the de-embedding task by either programming the required matrix operations in an element-by-element basis, or by taking full advantage of the available intrinsic linear algebra Matlab capabilities. Even though the choice is yours, please make sure to include a printout of your software as part of your laboratory report.

4. Use your Matlab code to provide plots of your de-embedded S-matrix results for the link between the two-monopoles', with $\ell = 500$ mm, and comment on what you are seeing.

   If needed, compare the S_{11} de-embedded results that you obtained in a previous laboratory with the current results, to confirm that you correctly implemented the de-embedding algorithm.

4 Friis' Formula

Observe that the above communication link calculations and measurements were performed without any restrictions on the distance ℓ between the two antennas; our methods work regardless of how large or how small ℓ is (the two antennas can even be in the near-zone of each other). However, in practice more often than not the distance ℓ is very, very large. In such cases Eq. 15 shows that $|Z_{21}| \approx 0$, as it is inversely proportional to ℓ (since $\vec{E}_1$ at the location of antenna 2 is proportional to $1/\ell$). This makes possible to simplify considerably Eq. 15 and therefore obtain a surprisingly simple result for the power transfer between two antennas. This approximation yields what is commonly referred to as the Friis' formula[5,6], a result so useful and simple that it is even suitable

[5]H. T. Friis,"A Note on a Simple Transmission Formula" Proc. of the I.R.E. and Waves and Electrons, May 1946, pp. 254–256.

[6]D. K. Cheng, *Field and Wave Electromagnetics*, Second edition, Addison-Wesley Pub. Co., 1989, Sec. 11-7.1.

for hand-held calculations. As a last task for this laboratory let's then take a good look at this very important formula.

Friis' formula assumes that no S_{21} phase information is needed and one is only interested in determining the maximum possible power that can be transferred between the two antennas located in free space. The Friis' formula derivation then assumes whatever is needed to assure this optimum power transfer, and hence provides an upper bound type of result. At first you may think that this may not be very useful. However, when implementing a communication link between two antennas it is of course good practice to maximize the power transfer, and hence closely approach the result provided by Friis' formula. Furthermore, if the two antennas are very far apart, phase information relative to a reference locally placed at the transmitter, as is done in VNA measurements (the zero phase corresponds to the phase of the signal at the calibration short circuit) is seldom possible or needed.

To maximize power transfer the two antennas must be properly oriented with respect to each other (e.g., as depicted in Fig. 1, for a link between dipoles) and also be very well matched to the input and output transmission lines. Recalling that $|Z_{21}| \approx 0$, the equivalent circuit of Fig. 2 shows that we then somehow need to make $Z_{11} = Z_0$ and $Z_{22} = Z_0$. With this Eq. 19 then reduces to

$$S_{21} = \frac{Z_{21}}{2Z_0}\,. \tag{57}$$

Now, recalling that in this matched case

$$S_{21} = \frac{V_2^-}{V_1^+}\,, \tag{58}$$

we obtain

$$|S_{21}|^2 = \frac{\frac{1}{2}|V_2^-|^2/Z_0}{\frac{1}{2}|V_1^+|^2/Z_0} = \frac{P_r}{P_t}\,, \tag{59}$$

where P_t and P_r are the powers provided to antenna 1 and delivered by antenna 2, respectively. Substituting Eq. 57 into Eq. 59 we then obtain

$$\frac{P_r}{P_t} = \left|\frac{Z_{21}}{2Z_0}\right|^2\,. \tag{60}$$

We will now proceed to obtain an approximation for $|Z_{21}|^2$ which, once substituted in Eq. 60, will yield what is referred to as Friis' formula.

Substituting Eq. 30 into Eq. 38 and observing that, since antenna 2 is far from antenna 1, the electric field produced by antenna 1 (i.e., E_{1z_2}) can be considered constant over the length of antenna 2, one obtains

$$Z_{21} = \frac{-1}{I_1 \sin(\beta_0 h_2)}\, E_{1z_2} \int_{-h_2}^{+h_2} \sin[\beta_0(h_2 - |z_2|)]\, dz_2\,. \tag{61}$$

Evaluating the above integral then yields

$$Z_{21} = \frac{1}{I_1 \sin(\beta_0 h_2)}\, E_{1z_2} \frac{2}{\beta_0}\, \left[\cos(\beta_0 h_2) - 1\right]\,. \tag{62}$$

Now, again recalling that we are working with large ℓ values, observe that Eq. 22 yields for the electric field $\vec{E}_2$, produced by antenna 2 at the location of antenna 1, the expression

$$\vec{E}_2 = \hat{z}_1 \, \frac{j\,\eta_0\, I_2}{4\pi \sin(\beta_0 h_2)} \, \frac{e^{-j\beta_0 \ell}}{\ell} \, 2\,[\cos(\beta_0 h_2) - 1] \; . \tag{63}$$

We can then divide Eq. 62 by the E_{2z_1} provided by Eq. 63 and obtain

$$Z_{21} = \frac{4\pi}{j\eta_0\beta_0} \, \frac{\ell}{e^{-j\beta_0\ell}} \, \frac{E_{1z_2}}{I_1} \, \frac{E_{2z_1}}{I_2} \, . \tag{64}$$

Before proceeding with the Friis' formula derivation observe that, since what is being called antennas 1 and 2 is arbitrary, the numbers 1 and 2 can be interchanged in Eq. 64 to yield

$$Z_{12} = \frac{4\pi}{j\eta_0\beta_0} \, \frac{\ell}{e^{-j\beta_0\ell}} \, \frac{E_{2z_1}}{I_2} \, \frac{E_{1z_2}}{I_1} \, , \tag{65}$$

and since the right side of Eqs. 65 and 64 are equal, it is clear that $Z_{12} = Z_{21}$. Note however that, even though $Z_{12} = Z_{21}$ for any ℓ value, in here we just confirmed that $Z_{12} = Z_{21}$ when the two antennas are far apart.

To finish our derivation of Friis' formula we now substitute Eq. 64 into Eq. 60 to obtain

$$\frac{P_r}{P_t} = \left(\frac{4\pi\ell}{\beta_0}\right)^2 \frac{1}{4} \, \frac{|E_{1z_2}|^2/(2\eta_0)}{\frac{1}{2}|I_1|^2 Z_0} \, \frac{|E_{2z_1}|^2/(2\eta_0)}{\frac{1}{2}|I_2|^2 Z_0} \, . \tag{66}$$

Finally recalling that, since the two antennas are assumed matched to the corresponding transmission lines,

$$P_t = \frac{1}{2}\,|I_1|^2 Z_0 \, , \tag{67}$$

$$P_r = \frac{1}{2}\,|I_2|^2 Z_0 \, , \tag{68}$$

and the gain definition yields[7]

$$\frac{|E_{1z_2}|^2}{2\eta_0} = \frac{P_t G_t}{4\pi\ell^2} \, , \tag{69}$$

$$\frac{|E_{2z_1}|^2}{2\eta_0} = \frac{P_r G_r}{4\pi\ell^2} \, , \tag{70}$$

Eq. 66 can be rewritten as the desired Friis' formula:

$$\frac{P_r}{P_t} = G_t \, G_r \left(\frac{\lambda_0}{4\pi\ell}\right)^2 . \tag{71}$$

Although the format used in Eq. 71 is what is usually shown in the literature as the Friis' formula, since it is convenient for computations, is is possible to write this equation is a slightly different way, one that more clearly shows how the communication link is operating, namely

$$P_r = P_t \; G_t \; \frac{1}{4\pi\ell^2} \; A_{eff} \, , \tag{72}$$

[7] D. K. Cheng, *Field and Wave Electromagnetics*, Second edition, Addison-Wesley Pub. Co., 1989, Sec. 11-3.

where

$$\boxed{A_{eff} = G_r \frac{\lambda_0^2}{4\pi}} \tag{73}$$

is the *effective area of the receiving antenna*. Eq. 73 is a fundamental result; it relates the transmitting (i.e., the gain) and receiving (i.e., the effective area) properties of an antenna to each other.

Sequentially considering from left to right the terms present on the right of the equal sign of Eq. 72, the power P_t is fed to the transmitting antenna, which concentrates it in the direction of the receiving antenna with a gain G_t. This power then proceeds to spread as it travels in free space towards the receiving antenna as a spherical wave (the area of the sphere that has the receiving antenna on its surface is $4\pi\ell^2$, and hence the term $1/(4\pi\ell^2)$ can be referred to as the *free-space decay factor*). The radiated power then finally arrives at the receiving antenna with a power density (in W/m^2) equal to $P_t\ G_t/(4\pi\ell^2)$. The receiving antenna then collects the part of this power density that falls into its effective area A_{eff}, and this becomes the received power P_r.

Equation 71 was derived specifically considering two dipole antennas (this fact came in through Eqs. 61 and 63). This was done in the interest of clarity, since this laboratory deals with dipole antennas. However, it is very important to point out that it is possible to carry out the derivation without resorting to specific antenna geometries (antennas 1 and 2 do not even need to be equal), and therefore show that Eqs. 72 and 73 (and hence Eq. 71) are actually general results, valid for any type of antennas.

By the way, Friis' formula requires that the two antennas be located in free space and with an unobstructed view of each other. Hence the case of a link between two monopoles on top of a infinite ground plane does not satisfy this assumption. However, it can be shown that the P_r/P_t result corresponding to this situation is just 1/4 of the result provided by Eq. 71.

Let's now see how Friis' formula can be successfully applied to the communication link that we calculated and measured in the previous section.

1. To start, what is the gain G_d of a half-wave long dipole? Provide your values in both linear and dB scales.

2. What is the gain G_m of a quarter-wave long monopole on a perfectly conducting ground plane of *infinite extent*? Provide your values in both linear and dB scales.

3. Augment the Matlab code that you generated in the previous section to also calculate and plot the $|S_{21}|$ provided by Friis' formula.

   Note that, to compare the two theoretical approaches, you will be needing the value of the gain of your monopoles with their *finite ground planes* (i.e., G_t and G_r). However, let's wait a bit before addressing this topic. For now, since it is convenient to both cement your understanding as well as for code debugging purposes, let's consider only the predictions for a link between the two half-wave dipoles (not two monopoles) previously designed for 600 MHz with $2a = 0.4$ mm.

   Observe that overall the predictions using Friis' formula are showing very large disagreements when compared to the predictions using the mutual impedance approach. However, at this point you should at least be seeing very good agreement

at the 600 MHz frequency, since we know that our antennas have been designed for, and hence work very well, at this frequency. We will address any observed disagreement away from 600 MHz in a subsequent item. For now let's concentrate only on predictions at 600 MHz.

By the way, if you are not seeing good agreement between the two predictions at 600 MHz you either have bugs in your code or it is being used incorrectly (e.g., is your code calculating and using the correct dipole S_{11}, S_{21}, and gain values?). Make sure to proceed to the next item only after you have good agreement at 600 MHz.

Please provide a plot of the $|S_{21}|$ of the dipole link, calculated using Friis' formula over the entire 50 kHz – 1.0 GHz frequency range, superimposed to the plot using the previously implemented mutual impedance calculation.

4. Any discrepancies observed in the $|S_{21}|$ result provided by Friis' formula, at 600 MHz, should by now have been successfully addressed in the previous item. However, away from this frequency discrepancies of the order of tens of dBs still remain, and hence can't be ignored.

   Since all the electrical lengths associated with the monopoles' dimensions depend on frequency, their radiation patterns also depend on frequency, and hence their gain. Perhaps then these changes are responsible for the massive disagreements observed away from 600 MHz. Since at first this may appear to be a reasonable working hypothesis, let's take a closer look at it. To this effect consider the radiation patterns of linear dipoles, and explain (in your laboratory report) why they are not changing excessively over our frequency range of interest[8]. Note that even the radiation pattern of a Hertz dipole, which has negligible electrical length, is very similar to the radiation pattern of a full-wave dipole. This important fact indicates that the gain of the monopoles' are quite stable with frequency, provided that their electrical dimensions stay under about a wavelength, which is the case of our monopoles over the 50 kHz – 1.0 GHz frequency range.

   The cause of the large $|S_{21}|$ discrepancies observed are then not due to a variation of antenna gain with frequency. A much more important effect is systematically not being captured by Frii's formula, because somehow this effect is not significant at the operation frequency of a well designed antenna. Using this clue can you think of what the effect is? If not, please go back to the above derivation of Friis' formula, take a another careful look at it (the answer is in there), and only move ahead after you have successfully determined what has been ignored.

   Please provide a plot of the $|S_{21}|$ of the dipole link, calculated using the revised Friis' formula over the entire 50 kHz – 1.0 GHz frequency range, superimposed to the plot using the previous implemented mutual impedance calculation. Your plot should now show excellent agreement between the two theoretical methods over the entire 50 kHz – 1.0 GHz frequency range.

[8]Check for example Fig. 11-6 of D. K. Cheng, *Field and Wave Electromagnetics*, Second edition, Addison-Wesley Pub. Co., 1989.

5. Let's now return to the link between two monopole antennas, which is what you have previously measured. Since the Friis' formula is currently using the gain values of half-wave dipoles, they have to be changed to use instead the monopole gain values.

   Use the gain value of a quarter-wave long monopole on a perfectly conducting ground plane of *infinite extent* in your calculations and take a look at how they compare (do not forget that the S_{11} and the S_{21} of the monopole are half the values calculated for the dipole).

   Perhaps to your surprise, observe that now the predicted values using the mutual impedance technique and the Frii's formula disagree significantly, even though the measured values agree well with the mutual impedance technique predictions.

6. The reason for the disagreement observed in the previous item rests on the fact that the monopoles' gain depend significantly on the size of their ground planes. You can find a large amount of information on this effect in the literature, as it has been observed and discussed since the early years of the twentieth century, and perhaps surprisingly continues to be revisited to this day[9].

   With the above in mind we will then approach the monopole gain in a reverse way. Since by now we know that we can trust the measurements and predictions obtained in the previous section, use Friis' formula to *measure* the gain G_m of your monopoles at 600 MHz, provide the measured value with your report, add the correct gain value to your Matlab code predictions, and provide the correspond plots with your report. By the way, and in case you are wondering, this procedure is actually how gain values are very precisely measured in practice. (Fig. 7 depict some typical results).

No matter how small the P_r of Eq. 71 becomes as ℓ increases, it is never zero, and it is this small value that renders the communication between two distant antennas possible. As an extreme example, engineers have been successfully using these exceeding small P_r values to communicate with spacecraft at the edge of our solar system, a communication feat over truly astronomical distances. What happens is that the $1/\ell$ proportionality associated with radiation actually yields a very slow field decay as the distance between the two antennas increases.

The above free-space decay with ℓ is way, way more benign that the exponential decay caused by the unavoidable attenuation of confined communications (e.g., transmission lines and optical fibers). To provide a comparison, a very high quality modern optical fiber is capable of yielding the impressively small attenuation $\alpha \approx 0.2$ dB/km, at the infrared communication wavelength of 1.55 μm. Even though this is quite a technological feat, it quickly adds up as the traveled distance increases. As an example, consider an underwater transatlantic optical cable connecting California to

[9]See for instance the values provided in Tab. 1 of Z. Živković, D. Senić, C. Bodendorf, J. Skrzypczynski, and A. Šarolić, "Radiation pattern and impedance of a quarter wavelength monopole antenna above a finite ground plane, " SoftCOM 2012, 20th International Conference on Software, Telecommunications and Computer Networks, 2012, pp. 1-5. They show that the gain of a monopole in a circular plane of $\sim 0.5\lambda_0$ radius is lower by about 3 dB from the infinite ground plane value.

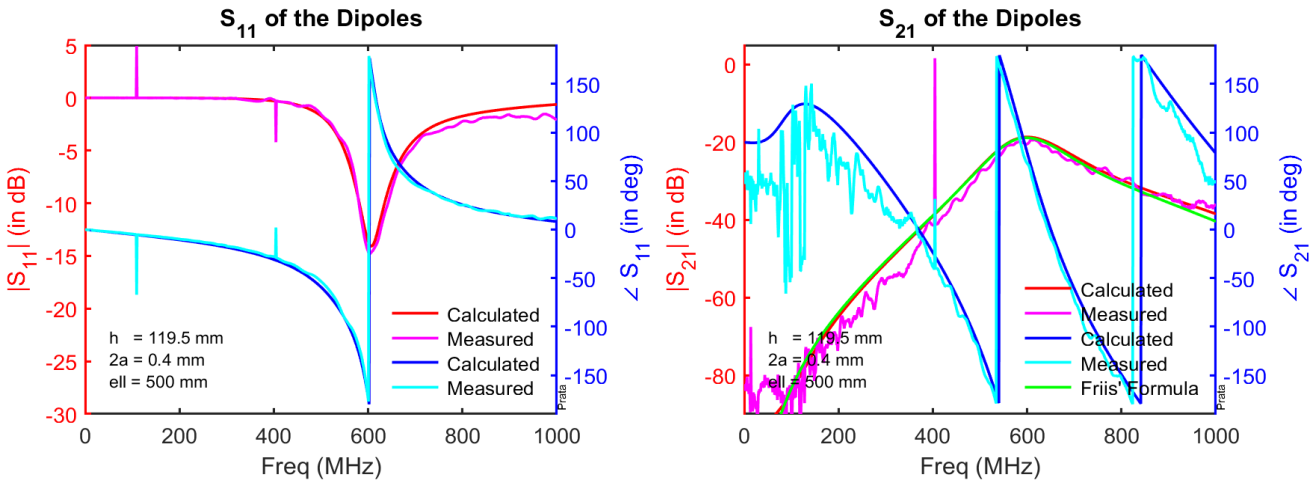

Figure 7: Typical monopole's link de-embedded S-parameter results

Hawaii. Since the corresponding distance is about 4,450 km, an whopping attenuation of $4{,}450 \times 0.2 = 890$ dB will result, and hence it is impossible to directly use an optical fiber to communicate between California and Hawaii. As a consequence, underwater transatlantic optical cables typically have to deal with no more than about 100 km spacing between the required regenerative signal repeaters, as the $100 \times 0.2 = 20$ dB is about the maximum that can be tolerated to maintain the needed signal quality for the required high-speed communication. In comparison NASA's Voyager 1 spacecraft, as of 2022 humankind's most distant operational spacecraft, has been flying for about 45 years and is currently around 156 astronomical units (i.e., AU) away from earth. Even though this corresponds to the incredible distance of $\ell = 23.3 \times 10^{12}$ m, the associated free-space decay present in Eq. 71 is $10\log(4\pi\ell^2) = 278$ dB. Although this is still a very large value, with the help of very large antennas (to provide very large gain values) and radiated power, and very low-noise receivers, radio communications with Voyager 1 continues to occur in 2022, albeit at very low data rates.